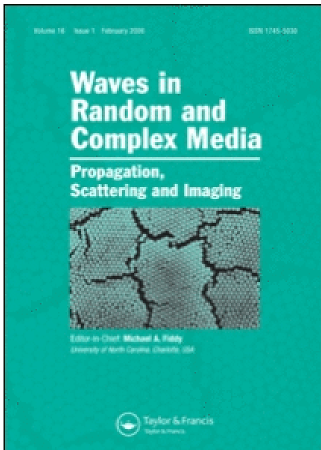

Waves in Random and Complex Media
Publication details, including instructions for authors and subscription information:
http://www.informaworld.com/smpp/title~content=t716100762

Unified boundary integral equation for the scattering of elastic and acoustic waves: solution by the method of moments

Mei Song Tong [a]; Weng Cho Chew [a]
[a] Department of Electrical and Computer Engineering, University of Illinois at Urbana-Champaign, Urbana, Illinois, USA

Online Publication Date: 01 May 2008

To cite this Article: Tong, Mei Song and Chew, Weng Cho (2008) 'Unified boundary integral equation for the scattering of elastic and acoustic waves: solution by the method of moments', Waves in Random and Complex Media, 18:2, 303 — 324

To link to this article: DOI: 10.1080/17455030701798960
URL: http://dx.doi.org/10.1080/17455030701798960

Waves in Random and Complex Media
Vol. 18, No. 2, May 2008, 303–324

Unified boundary integral equation for the scattering of elastic and acoustic waves: solution by the method of moments

Mei Song Tong and Weng Cho Chew*

Department of Electrical and Computer Engineering, University of Illinois at Urbana-Champaign, Urbana, Illinois, USA

(*Received 8 September 2007; final version received 7 October 2007*)

A unified boundary integral equation (BIE) is developed for the scattering of elastic and acoustic waves. Traditionally, the elastic and acoustic wave problems are solved separately with different BIEs. The elastic wave case is represented in a vector BIE with the traction and displacement vectors as unknowns whereas the acoustic wave case is governed by a scalar BIE with velocity potential or pressure as unknowns. Although these two waves can be unified in the form of a partial differential equation, the unified form in its BIE counterpart has not been reported. In this work, we derive the unified BIE for these two waves and then show that the acoustic wave case can be derived from this BIE by introducing a shielding loss for small shear modulus approximation; hence only one code needs to be maintained for both elastic and acoustic wave scattering. We also derive the asymptotic Green's tensor for zero shear modulus and solve the corresponding vector equation. We employ the method of moments, which has been widely used in electromagnetics, as a numerical tool to solve the BIEs involved. Our numerical experiments show that it can also be used robustly in elastodynamics and acoustics.

1. Introduction

The study of elastic or acoustic wave behaviour requires solving the corresponding wave equations. These equations can be in the form of a partial differential equation (PDE) or a boundary integral equation (BIE). It is very clear that the acoustic wave equation is a special case of the elastic wave equation and they can be solved in a unified form as a PDE [1–3]. Conventionally, however, the elastic wave BIE and the acoustic wave BIE are treated differently [4, 5]. This is because the acoustic wave BIE has a simpler form and it is unnecessary to resort to solving the full-fledged elastic wave BIE in most cases. In this work, we unify the acoustic wave BIE and elastic wave BIE and show that the acoustic wave case can be obtained as a special case of the full elastic wave BIE. Our unified BIE provides a new approach to solve those problems in a more versatile manner. This is accomplished by introducing a shielding loss for a small shear modulus in the elastic wave BIE and solving it as an elastic wave problem. This shielding loss attenuates the shear wave in the medium. The advantage of this approach is that it requires the maintenance of only one numerical code that can account for both elastic wave physics and acoustic wave physics. This is especially important for modern day computational engineering where numerical codes for complex structures often require high maintenance due to the complexity of the codes.

*Corresponding author. Currently on leave from UIUC to serve at The University of Hong Kong. Email: w-chew@uiuc.edu

ISSN: 1745-5030 print / 1745-5049 online

DOI: 10.1080/17455030701798960
http://www.informaworld.com

This work fills a void in the numerical elastic scattering solutions for integral equation solvers where the acoustic wave scattering is never derived from a full-fledged code for elastic wave scattering, even though it has been done in differential equation solvers. Furthermore, we also derive the asymptotic Green's function and the BIE for the $\mu \to 0$ case, where μ is the shear modulus of the host medium, and solve the corresponding vector BIE. The new approach has the same complexity as the traditional acoustic wave BIE, but can provide extra information about the displacement field in addition to the potential in its solution.

In acoustics, one usually works with the velocity potential or pressure as the unknowns leading to a simpler scalar BIE. If the obstacle is soft or elastic, the surface impedance concept is used to account for the property of the obstacle. However, for fluid or underwater acoustics problems, the traditional scalar acoustic wave BIE may not be appropriate; hence one has to resort to the vector elastic wave BIE with displacement and stress vectors as unknowns [6–8].

We choose the method of moments (MoM) as a numerical tool to solve the unified BIE. MoM, similar to Galerkin's method, is a very robust numerical method that has been used in electromagnetics and has also been introduced to solve for the scalar acoustic BIE [9–14]. MoM expands the unknown functions in a BIE using basis functions and tests the resultant BIE using weighting functions to form algebraic matrix equations. Compared with collocation-based methods, such as the boundary element method (BEM) and the Nyström method, MoM enforces the boundary conditions to be satisfied over an element in an average sense, and minimizes or controls the weighted residue error in a better philosophy [10]. If the weighting function is the same as the basis function, it is known as Galerkin's method. Both MoM and Galerkin's method have been used to solve the scalar acoustic BIE [9–18], but have not been implemented yet for the vector elastic wave BIE.

Since the elastic wave BIE has 3D unknown vectors over a boundary surface, the implementation of MoM is not straightforward compared with electromagnetic BIEs. We have to separate the unknown vectors into tangential components and normal components along the surface and expand them in basis functions individually. We choose the Rao–Wilton–Glisson (RWG) basis [19] to represent the tangential components and pulse basis to represent the normal components. These basis functions are also used as the weighting function to test the BIE, resulting in a Galerkin process.

In the numerical process for the unified acoustic wave BIE, we will encounter the integral kernels with $1/R^3$ singularity, where R is the distance between a field point and a source point. This singularity is generated from the double gradient of the scalar compressional wave Green's function. In elastic wave scattering, the shear wave exists and this singularity is cancelled by the same term in the double gradient of the scalar shear wave Green's function, leading to an easily handled $1/R^2$ singularity.

In the acoustic wave problem, the shear wave vanishes and the degree of singularity increases to $1/R^3$. This may have been a challenging problem before, but we have developed a technique based on the Cauchy principal value (CPV) to treat these kinds of singular integrals in electromagnetics [20], and the same procedure can be followed here.

This paper is organized as follows. In Section 2, we describe the original BIE for elastic wave scattering developed by Pao and Varatharajulu [21]. In Section 3, we derive the limit of the dyadic Green's function in the BIE for acoustic waves. In Section 4, the unified BIE for acoustic waves is developed and the equivalence to the conventional scalar BIE is proved. Section 5 introduces MoM and illustrates its use for the elastic wave BIE and unified acoustic wave BIE. Section 6 presents numerical examples either for elastic waves or for acoustic waves to illustrate the applications of the MoM and unified BIE. Finally, we draw some conclusions in Section 7.

2. Elastic wave BIE

Consider the scattering of an elastic wave by a homogeneous obstacle V_0 with boundary S, as shown in Figure 1. The obstacle, whose properties are characterized by the mass density ρ_0 and Lamé constants λ_0 and μ_0, is embedded in an infinite 3D isotropic elastic medium V. Here we use the subscript 0 to indicate the parameters of the obstacle. Similarly, the host medium is characterized by ρ, λ and μ with no subscript for its parameters. The coordinate system is labelled in indicial notation (x_1, x_2, x_3) corresponding to (x, y, z) for convenience.

The incident wave is a time-harmonic compressional (longitudinal) plane wave propagating along the $-x_3$ direction and impinging upon the obstacle. If we incorporate boundary conditions which are the continuity of displacement and traction vectors, the BIE can be written as [21]

$$\frac{1}{2}\mathrm{u}(\mathrm{x}) + \int_S [\overline{\mathrm{R}}^T(\mathrm{x}, \mathrm{x}') \cdot \mathrm{u}(\mathrm{x}') - \overline{\mathrm{G}}^T(\mathrm{x}, \mathrm{x}') \cdot \mathrm{t}(\mathrm{x}')]\, dS' = \mathrm{u}^I(\mathrm{x}), \quad \mathrm{x} \in S$$

$$\frac{1}{2}\mathrm{u}(\mathrm{x}) + \int_S [\overline{\mathrm{G}}_0^T(\mathrm{x}, \mathrm{x}') \cdot \mathrm{t}(\mathrm{x}') - \overline{\mathrm{R}}_0^T(\mathrm{x}, \mathrm{x}') \cdot \mathrm{u}(\mathrm{x}')]\, dS' = 0, \quad \mathrm{x} \in S \tag{1}$$

where u and t, the unknowns to be solved, are the total displacement and traction vectors at the surface of the obstacle. $\overline{\mathrm{G}}$ is the dyadic Green's function given by

$$\overline{\mathrm{G}} = \frac{1}{\mu}\left(\bar{\mathrm{I}} + \frac{\nabla\nabla}{\kappa_s^2}\right) g_s(\mathrm{x}, \mathrm{x}') - \frac{1}{\gamma}\frac{\nabla\nabla}{\kappa_c^2} g_c(\mathrm{x}, \mathrm{x}') \tag{2}$$

and $\overline{\mathrm{R}} = \hat{\mathrm{n}}' \cdot \overline{\overline{\Sigma}}(\mathrm{x}, \mathrm{x}')$ where $\overline{\overline{\Sigma}}(\mathrm{x}, \mathrm{x}') = \lambda\bar{\mathrm{I}}\nabla \cdot \overline{\mathrm{G}} + \mu(\nabla\overline{\mathrm{G}} + \overline{\mathrm{G}}\nabla)$ is a third-rank Green's tensor. The superscript T on $\overline{\mathrm{G}}$ and $\overline{\mathrm{R}}$ denotes the transpose which can be removed if their positions with the vector u or t are exchanged. The constant $\frac{1}{2}$ in front of $\vec{u}$ follows from the assumption that the observation point is on a locally smooth surface on S. Note that the integrals in all BIEs are defined in the CPV sense.

In Equation (2), $g_s = e^{i\kappa_s R}/4\pi R$ and $g_c = e^{i\kappa_c R}/4\pi R$ are the scalar Green's functions in free space with $R = |\mathrm{x} - \mathrm{x}'|$ being the distance between the field point x and the source point x′. The subscript s denotes the shear wave and c denotes the compressional wave. The corresponding wave numbers are given by $\kappa_s^2 = \omega^2\rho/\mu$ and $\kappa_c^2 = \omega^2\rho/\gamma$ with $\gamma = \lambda + 2\mu$. In addition, the superscript I in (1) denotes an incident wave, a single bar over a vector denotes a dyadic tensor,

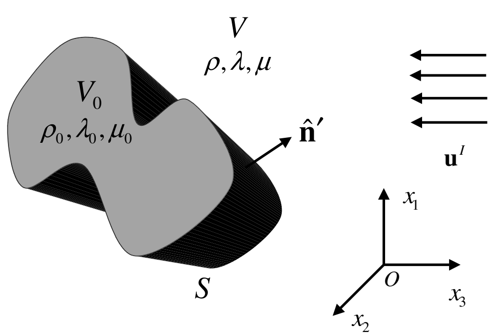

Figure 1. Elastic wave scattering by an arbitrarily-shaped homogeneous obstacle embedded in an infinite 3D isotropic elastic medium.

double bars over a vector denote a third-rank tensor and $\bar{\text{I}}$ stands for the identity dyadic tensor in (1) and (2). $\overline{\text{G}}$ and $\overline{\text{R}}$ are also known as the Stokes displacement tensor and traction tensor, respectively, and their expressions in indicial notation can be found in many publications [22, 23].

If the obstacle is a traction-free cavity, then the total traction on the surface vanishes and the above equations reduce to

$$\frac{1}{2}\text{u}(\text{x}) + \int_S \overline{\text{R}}^T(\text{x}, \text{x}') \cdot \text{u}(\text{x}')\, dS' = \text{u}^I(\text{x}), \quad \text{x} \in S. \tag{3}$$

If the obstacle is a fixed rigid inclusion, then the total displacement on the surface vanishes and the above equations reduce to

$$\int_S \overline{\text{G}}^T(\text{x}, \text{x}') \cdot \text{t}(\text{x}')\, dS' = -\text{u}^I(\text{x}), \quad \text{x} \in S. \tag{4}$$

As we mentioned above, there is a numerical difficulty in solving for the BIE when $\mu \to 0$ in the host medium. However, if we introduce a loss for the host medium that causes the shear wave to decay quickly, then we can solve the pertinent BIE. This can be accomplished by choosing a small negative value for μ to approximate the original positive value of μ. After doing so, the wave number $\kappa_s = \omega\sqrt{\rho/\mu}$ will have a large imaginary part with a chosen plus sign. The Green's function now decays exponentially like an evanescent wave with no oscillatory behaviour. Then the integration with $e^{i\kappa_s R}$ in the kernel is no longer difficult. The approach will give us a good approximate solution for the small value of μ as demonstrated in the numerical examples.

3. Limit of dyadic Green's function

For acoustic waves, there is no shear wave propagating in the surrounding non-viscous medium and $\mu = 0$. The limit of the dyadic Green's function $\overline{\text{G}}$ when $\mu \to 0$ in the host medium may not be derived from its explicit expression (2). When $\mu \to 0$, $\kappa_s \to \infty$ and the scalar shear Green's function g_s becomes highly oscillatory. This high oscillation makes numerical computation with this Green's function difficult in this limit. Hence, there is no direct way to calculate the asymptotic dyadic Green's function. However, a highly oscillatory integrand including ê{ik_sR} in wave physics, when integrated, contributes a small value to the integral eventually when k_s is very large. This is because the alternating positive and nagative values of the integrand within an interval will be mostly cancelled each other and the residue will be very small when k_s is very large. Therefore, we can derive the limit by inspecting the derivation of the dyadic Green's function using the Fourier–Laplace transform [24].

The elastic wave equation in PDE form is

$$(\lambda + \mu)\nabla\nabla \cdot \text{u} + \mu\nabla^2\text{u} - \rho\ddot{\text{u}} = -\text{f}. \tag{5}$$

Applying the Fourier–Laplace transform

$$\text{u}(\text{x}, t) = \frac{1}{(2\pi)^4}\int_{-\infty}^{\infty} d\omega e^{-i\omega t}\int_{-\infty}^{\infty} d\text{k}e^{\text{ik}\cdot\text{x}}\tilde{\text{u}}(\text{k}, \omega) \tag{6}$$

we obtain

$$\begin{aligned}\tilde{\mathrm{u}}(\mathrm{k},\omega) &= [(\lambda+\mu)\mathrm{kk}+\mu\kappa^2\bar{\mathrm{I}}-\omega^2\rho\bar{\mathrm{I}}]^{-1}\cdot\tilde{\mathrm{f}}(\mathrm{k},\omega)\\ &= (\alpha\bar{\mathrm{I}}+\beta\mathrm{kk})\cdot\tilde{\mathrm{f}}(\mathrm{k},\omega)\\ &= \left(\bar{\mathrm{I}}-\frac{\mathrm{k}}{\mathrm{k}}\kappa_s^2\right)\cdot\frac{\tilde{\mathrm{f}}(\mathrm{k},\omega)}{\mu\left(\kappa^2-\kappa_s^2\right)}+\frac{\mathrm{kk}\cdot\tilde{\mathrm{f}}(\mathrm{k},\omega)}{\kappa_c^2\gamma\left(\kappa^2-\kappa_c^2\right)}\end{aligned} \tag{7}$$

where

$$\begin{aligned}\alpha &= \frac{1}{\mu\kappa^2-\omega^2\rho}\\ \beta &= -\frac{1}{\kappa_s^2\mu\left(\kappa^2-\kappa_s^2\right)}+\frac{1}{\kappa_c^2\gamma\left(\kappa^2-\kappa_c^2\right)}.\end{aligned} \tag{8}$$

If $\mu \neq 0$ which is the elastic wave case, it can be shown that

$$\begin{aligned}\int_{-\infty}^{\infty} d\mathrm{k}e^{ik\cdot x}\left(\bar{\bar{I}}-\frac{\mathrm{kk}}{\kappa_s^2}\right)\frac{1}{\mu\left(\kappa^2-\kappa_s^2\right)} &= \left(\bar{\mathrm{I}}+\frac{\nabla\nabla}{\kappa_s^2}\right)\frac{g_s}{\mu}\\ \int_{-\infty}^{\infty} d\mathrm{k}e^{i\mathrm{k}\cdot\mathrm{x}}\frac{\mathrm{kk}}{\kappa_c^2\gamma\left(\kappa^2-\kappa_c^2\right)} &= -\frac{\nabla\nabla}{\kappa_c^2}\frac{g_c}{\gamma}\end{aligned} \tag{9}$$

yielding the dyadic Green's function as shown in (2). However, the first Equation in (9) is not valid if $\mu = 0$ which is the acoustic wave case. This is because the identity used in deriving that equation

$$\int_{-\infty}^{\infty}\frac{d\mathrm{k}e^{i\mathrm{k}\cdot\mathrm{x}}}{\kappa^2-\kappa_s^2} = -g_s \tag{10}$$

is not well-defined as in the lossless medium case in electromagnetics [25]. In fact, when $\mu = 0$, (8) is reduced to

$$\begin{aligned}\alpha &= -\frac{1}{\omega^2\rho}\\ \beta &= \frac{1}{\kappa_c^2\lambda\left(\kappa^2-\kappa_c^2\right)}.\end{aligned} \tag{11}$$

and the first Equation in (9) becomes

$$\begin{aligned}\lim_{\mu\to 0}\int_{-\infty}^{\infty} d\mathrm{k}e^{i\mathrm{k}\cdot\mathrm{x}}\left(\bar{\mathrm{I}}-\frac{\mathrm{kk}}{\kappa_s^2}\right)\frac{1}{\mu\left(\kappa^2-\kappa_s^2\right)} &= -\frac{\bar{\mathrm{I}}}{\omega^2\rho}\int_{-\infty}^{\infty} d\mathrm{k}e^{i\mathrm{k}\cdot\mathrm{x}}\\ &= -\frac{\delta(\mathrm{x}-\mathrm{x}')}{\omega^2\rho}\cdot\bar{\mathrm{I}}\end{aligned} \tag{12}$$

where $\delta(\mathrm{x}-\mathrm{x}')$ is the Dirac delta function. Hence, the limit of the dyadic Green's function for $\mu = 0$ is

$$\overline{\mathrm{G}}(\mathrm{x},\mathrm{x}') = -\frac{1}{\omega^2\rho}[\delta(\mathrm{x}-\mathrm{x}')\bar{\mathrm{I}} + \nabla\nabla g_c(\mathrm{x},\mathrm{x}')]. \quad (13)$$

4. Vector BIE for acoustic wave

It is of interest to obtain the limit of the dyadic Green's function for acoustic waves when $\mu \to 0$. Having the asymptotic Green's function in (13), the other related quantities can be simplified with $\mu = 0$ as follows

$$\begin{aligned}
\mathrm{t}(\mathrm{x}') &= \hat{\mathrm{n}}' \cdot \{\lambda\bar{\mathrm{I}}\nabla' \cdot \mathrm{u}(\mathrm{x}') + \mu[\nabla'\mathrm{u}(\mathrm{x}') + \mathrm{u}(\mathrm{x}')\nabla']\} \\
&= \hat{\mathrm{n}}'[\lambda\nabla' \cdot \mathrm{u}(\mathrm{x}')] \\
\mathrm{R}(\mathrm{x},\mathrm{x}') &= \hat{\mathrm{n}}' \cdot \{\lambda\bar{\mathrm{I}}\nabla \cdot \overline{\mathrm{G}}(\mathrm{x},\mathrm{x}') + \mu[\nabla\overline{\mathrm{G}}(\mathrm{x},\mathrm{x}') + \overline{\mathrm{G}}(\mathrm{x},\mathrm{x}')\nabla]\} \\
&= \hat{\mathrm{n}}'\nabla g_c(\mathrm{x},\mathrm{x}') \quad (14)
\end{aligned}$$

and the first Equation in (1) becomes

$$\begin{aligned}
&\int_S \{[-\lambda\nabla' \cdot \mathrm{u}(\mathrm{x}')]\hat{\mathrm{n}}' \cdot \overline{\mathrm{G}}(\mathrm{x},\mathrm{x}') + \mathrm{u}(\mathrm{x}') \cdot [\hat{\mathrm{n}}'\nabla g_c(\mathrm{x},\mathrm{x}')]\}dS' \\
&= -\frac{1}{2}\mathrm{u}(\mathrm{x}) + \mathrm{u}^I(\mathrm{x}) \quad \mathrm{x} \in S. \quad (15)
\end{aligned}$$

where we have removed the transpose on the kernels by exchanging their order with u or t for convenience. This is a vector BIE for acoustic waves. This vector BIE is a limiting case of the elastic wave BIE and can be solved with the second equation in (1).

Notice that the boundary conditions here may be different from before and can be expressed as [6]

$$\begin{aligned}
\hat{\mathrm{n}} \cdot \mathrm{u}_+ &= \hat{\mathrm{n}} \cdot \mathrm{u}_- \\
\hat{\mathrm{n}} \cdot \mathrm{t}_+ &= \hat{\mathrm{n}} \cdot \mathrm{t}_- \\
\hat{\mathrm{n}} \times \mathrm{t}_- &= 0 \quad (16)
\end{aligned}$$

where $+$ and $-$ implies that the observation points approach the boundary surface from the exterior and interior of the obstacle, respectively. These conditions state that the normal components of the displacement and traction vectors are continuous and the tangential component of the traction vector vanishes (also continuous), but the tangential component of the displacement may not be continuous at the surface due to the assumption that the host medium may be non-viscous [26].

In fact, the above vector BIE is equivalent to the conventional scalar acoustic wave BIE. If we take a divergence on the vector BIE and define the potential $\Phi = \nabla \cdot \mathrm{u}$, we have

$$\begin{aligned}
&\int_S \{-\lambda\Phi(\mathrm{x}')\nabla \cdot [\hat{\mathrm{n}}' \cdot \overline{\mathrm{G}}(\mathrm{x},\mathrm{x}')] + \mathrm{u}(\mathrm{x}') \cdot \hat{\mathrm{n}}'\nabla^2 g_c(\mathrm{x},\mathrm{x}')\}dS' \\
&= -\frac{1}{2}\Phi(\mathrm{x}) + \Phi^I(\mathrm{x}) \quad \mathrm{x} \in S. \quad (17)
\end{aligned}$$

Since

$$\nabla \cdot [\hat{n}' \cdot \overline{G}(x, x')] = \nabla \cdot \overline{G}(x, x') \cdot \hat{n}'$$
$$= \frac{1}{\lambda} \nabla' g_c(x, x') \cdot \hat{n}' \tag{18}$$

and

$$\nabla^2 g_c(x, x') = -\kappa_c^2 g_c(x, x') - \delta(x - x') \tag{19}$$

with $\delta(x - x') = 0$ due to the CPV definition, we can write (17) as

$$\int_S [-\Phi(x')\hat{n}' \cdot \nabla' g_c(x, x') - u(x') \cdot \hat{n}' \kappa_c^2 g_c(x, x')] dS'$$
$$= -\frac{1}{2}\Phi(x) + \Phi^i(x) \quad x \in S. \tag{20}$$

Also, when $\mu = 0$, the elastic wave equation in PDE form reduces to

$$\nabla' \nabla' \cdot u(x') + \kappa_c^2 u(x') = 0 \tag{21}$$

or

$$\hat{n}' \cdot u(x') = -\frac{1}{\kappa_c^2} \hat{n}' \cdot \nabla' \nabla' \cdot u(x')$$
$$= -\frac{1}{\kappa_c^2} \hat{n}' \cdot \nabla' \Phi(x'). \tag{22}$$

Using (22) in (20), we obtain

$$\int_S [-\Phi(x')\hat{n}' \cdot \nabla' g_c(x, x') + \hat{n}' \cdot \nabla' \Phi(x') g_c(x, x')] dS'$$
$$= -\frac{1}{2}\Phi(x) + \Phi^i(x) \quad x \in S \tag{23}$$

which is consistent with the conventional scalar acoustic wave BIE.

The derivation above indicates that we can use the vector BIE (15) to solve for acoustic wave problems. The vector BIE is a special case of the elastic wave BIE and the solution for it will provide additional information about the displacement in addition to the potential if compared with the conventional scalar BIE. The potential is included in the traction vector in this case ($t = \hat{n}'[\lambda \nabla' \cdot u] = \hat{n}' \lambda \Phi$).

5. Method of moments

To illustrate MoM for solving the elastic or acoustic wave scattering solution in the vector BIE, we consider the BIE in (4) describing the scattering by a rigid obstacle. The general case is a natural extension of the example shown here.

As the first step in MoM, we separate the unknown traction vector into tangential and normal components, i.e.

$$\mathrm{t}(\mathrm{x}') = \mathrm{t}_t(\mathrm{x}') + \mathrm{t}_n(\mathrm{x}'). \tag{24}$$

We then expand the two components using RWG and pulse bases, respectively

$$\begin{aligned} \mathrm{t}_t(\mathrm{x}') &= \sum_{n=1}^{N_t} \alpha_n \mathrm{f}_n(\mathrm{x}') \\ \mathrm{t}_n(\mathrm{x}') &= \sum_{n=1}^{N_n} \beta_n \hat{\mathrm{n}}_n(\mathrm{x}'). \end{aligned} \tag{25}$$

In the above, $\mathrm{f}_n(\mathrm{x}')$ is the RWG basis as shown in Figure 2, $\hat{\mathrm{n}}_n(\mathrm{x}')$ is the unit normal vector of the nth triangle patch used as a pulse basis, and α_n and β_n represent the unknown expansion coefficients to be solved. The RWG basis is defined as [19]

$$\mathrm{f}_n(\mathrm{x}') = \begin{cases} \frac{\ell_n}{2S_n^+} \Lambda_n^+(\mathrm{x}') & \mathrm{x}' \in S_n^+ \\ \frac{\ell_n}{2S_n^-} \Lambda_n^-(\mathrm{x}') & \mathrm{x}' \in S_n^- \\ 0 & \text{otherwise} \end{cases} \tag{26}$$

where ℓ_n is the length of the common edge of two neighbouring triangles, S_n^+ and S_n^- are the areas of the two triangles, and $\Lambda_n^+(\mathrm{x}')$ and $\Lambda_n^-(\mathrm{x}')$ are the distance vectors as indicated in Figure 2. We have in total N_t non-boundary edges connecting two neighbouring triangles in which the RWG bases are defined and N_n triangles in which the pulse bases are defined.

After using the above expansion, the BIE can be written as

$$\sum_{n=1}^{N_t} \alpha_n \int_{S_n} \overline{\mathrm{G}}(\mathrm{x}, \mathrm{x}') \cdot \mathrm{f}_n(\mathrm{x}')\, dS' + \sum_{n=1}^{N_n} \beta_n \int_{S_n} \overline{\mathrm{G}}(\mathrm{x}, \mathrm{x}') \cdot \hat{\mathrm{n}}_n(\mathrm{x}')\, dS' = -\mathrm{u}^I(\mathrm{x}). \tag{27}$$

where we have omitted the transpose T on $\overline{\mathrm{G}}(\mathrm{x}, \mathrm{x}')$ without changing the order with t. This is because $\overline{\mathrm{G}}(\mathrm{x}, \mathrm{x}')$ is symmetrical [22].

The next step is using the basis functions as the weighting or testing functions to test the equation. By doing so, the following matrix equations are formed

$$\begin{aligned} \sum_{n=1}^{N_t} \alpha_n A_{mn} + \sum_{n=1}^{N_n} \beta_n B_{mn} &= E_{mn} \quad m = 1, \cdots, N_t \\ \sum_{n=1}^{N_t} \alpha_n C_{mn} + \sum_{n=1}^{N_n} \beta_n D_{mn} &= F_{mn} \quad m = 1, \cdots, N_n \end{aligned} \tag{28}$$

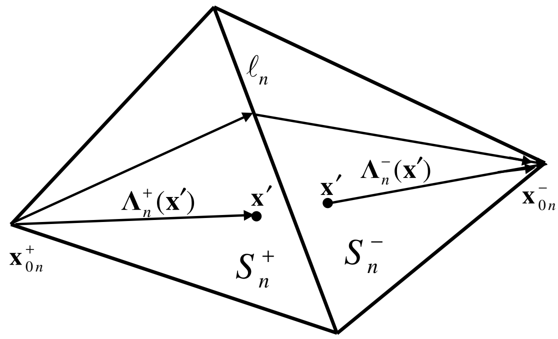

Figure 2. RWG basis f_n defined in two neighbouring triangles S_n^+ and S_n^-. These two triangles share the nth non-boundary edge whose length is ℓ_n. S_n^+ and S_n^- also denote the corresponding areas of the two triangles.

where

$$\begin{aligned}
A_{mn} &= \langle \mathrm{f}_m(\mathrm{x}), \overline{\mathrm{G}}(\mathrm{x},\mathrm{x}'), \mathrm{f}_n(\mathrm{x}')\rangle \\
&= \frac{\ell_m\ell_n}{4S_m^+S_n^+}\langle \Lambda_m^+(\mathrm{x}), \overline{\mathrm{G}}(\mathrm{x},\mathrm{x}'), \Lambda_n^+(\mathrm{x}')\rangle \\
&\quad + \frac{\ell_m\ell_n}{4S_m^+S_n^-}\langle \Lambda_m^+(\mathrm{x}), \overline{\mathrm{G}}(\mathrm{x},\mathrm{x}'), \Lambda_n^-(\mathrm{x}')\rangle \\
&\quad + \frac{\ell_m\ell_n}{4S_m^-S_n^+}\langle \Lambda_m^-(\mathrm{x}), \overline{\mathrm{G}}(\mathrm{x},\mathrm{x}'), \Lambda_n^+(\mathrm{x}')\rangle \\
&\quad + \frac{\ell_m\ell_n}{4S_m^-S_n^-}\langle \Lambda_m^-(\mathrm{x}), \overline{\mathrm{G}}(\mathrm{x},\mathrm{x}'), \Lambda_n^-(\mathrm{x}')\rangle \\
B_{mn} &= \langle \mathrm{f}_m(\mathrm{x}), \overline{\mathrm{G}}(\mathrm{x},\mathrm{x}'), \hat{\mathrm{n}}_n(\mathrm{x}')\rangle \\
&= \frac{\ell_m}{2S_m^+}\langle \Lambda_m^+(\mathrm{x}), \overline{\mathrm{G}}(\mathrm{x},\mathrm{x}'), \hat{\mathrm{n}}_n(\mathrm{x}')\rangle + \frac{\ell_m}{2S_m^-}\langle \Lambda_m^-(\mathrm{x}), \overline{\mathrm{G}}(\mathrm{x},\mathrm{x}'), \hat{\mathrm{n}}_n(\mathrm{x}')\rangle \\
C_{mn} &= \langle \hat{\mathrm{n}}_m(\mathrm{x}), \overline{\mathrm{G}}(\mathrm{x},\mathrm{x}'), \mathrm{f}_n(\mathrm{x}')\rangle \\
&= \frac{\ell_n}{2S_n^+}\langle \hat{\mathrm{n}}_m(\mathrm{x}), \overline{\mathrm{G}}(\mathrm{x},\mathrm{x}'), \Lambda_n^+(\mathrm{x}')\rangle + \frac{\ell_n}{2S_n^-}\langle \hat{\mathrm{n}}_m(\mathrm{x}), \overline{\mathrm{G}}(\mathrm{x},\mathrm{x}'), \Lambda_n^-(\mathrm{x}')\rangle \\
D_{mn} &= \langle \hat{\mathrm{n}}_m(\mathrm{x}), \overline{\mathrm{G}}(\mathrm{x},\mathrm{x}'), \hat{\mathrm{n}}_n(\mathrm{x}')\rangle \\
E_{mn} &= -\langle \mathrm{f}_m(\mathrm{x}), \mathrm{u}^I(\mathrm{x})\rangle \\
&= -\frac{\ell_m}{2S_m^+}\langle \Lambda_m^+(\mathrm{x}), \mathrm{u}^I(\mathrm{x})\rangle - \frac{\ell_m}{2S_m^-}\langle \Lambda_m^-(\mathrm{x}), \mathrm{u}^I(\mathrm{x})\rangle \\
F_{mn} &= -\langle \hat{\mathrm{n}}_m(\mathrm{x}), \mathrm{u}^I(\mathrm{x})\rangle
\end{aligned} \tag{29}$$

with

$$\begin{aligned}
\Lambda_n^+(\mathrm{x}') &= \mathrm{x}' - \mathrm{x}_{0n}^+ \\
\Lambda_n^-(\mathrm{x}') &= \mathrm{x}_{0n}^- - \mathrm{x}'.
\end{aligned} \tag{30}$$

The involved inner products above are defined, for example, as

$$\langle \mathrm{f}_m(\mathrm{x}), \overline{\mathrm{G}}(\mathrm{x}, \mathrm{x}'), \mathrm{f}_n(\mathrm{x}')\rangle = \int_{S_m} dS \mathrm{f}_m(\mathrm{x}) \cdot \int_{S_n} \overline{\mathrm{G}}(\mathrm{x}, \mathrm{x}') \cdot \mathrm{f}_n(\mathrm{x}')\, dS'$$

$$\langle \mathrm{f}_m(\mathrm{x}), \mathrm{u}^I(\mathrm{x})\rangle = \int_{S_m} \mathrm{f}_m(\mathrm{x}) \cdot \mathrm{u}^I(\mathrm{x})\, dS. \qquad (31)$$

The main work in MoM is the evaluation of these two-fold integrals to generate the system matrix. For elastic wave scattering, the integral kernels have only $1/R$ and $1/R^2$ singularities for singular elements and they can be easily handled. For acoustic wave scattering, however, there is a $1/R^3$ singularity in the evaluation of integrals for singular elements and we use the strategy developed in electromagnetics to perform these kinds of singular integrations [20]. To reduce the overhead of numerical integrations, the one-point quadrature rule can be used for the outer integrals in the testing procedure. Since the unknown coefficients in the RWG basis expansions are counted in terms of the non-boundary edges connecting two neighbouring triangles, MoM uses fewer unknowns compared with the collocation-based methods in the same mesh size.

6. Numerical results

6.1. *Elastic wave scattering*

To demonstrate the use of MoM in elastodynamics, we first consider scattering by a fixed rigid sphere with a radius of $a = 1.0$. The host medium has Poisson's ratio $\nu = 0.25$ and mass density $\rho = 1.0$. The incident wave has a unit circular frequency ($\omega = 1.0$) and normalized wave number of $\kappa_c a = 0.125$, 0.913 and π, respectively. Figures 3–5 show the radial and tangential (elevated) components of the total traction along the principal cut ($\phi = 0^\circ$ and $\theta = 0^\circ \sim 180^\circ$) at the surface. The surface is discretized into 960 flat triangles in all cases and may be overly meshed for the spheres of small sizes. It can be seen that the solutions agree with the analytical solutions very well. Note that the analytical solutions for general elastic wave scattering by a sphere can be found in [26], but the asymptotic solutions with $\mu \to 0$ for acoustic wave scattering are not available and we have derived them in the appendix.

We then consider the scattering in an elastic medium by a traction-free spherical cavity (void). The cavity has a radius of $a = 1.0$ and the host medium is characterized by Poisson's ratio $\nu = 1/3$, Young's modulus $E = 2/3$ and mass density $\rho = 1.0$. The incident wave has unit circular frequency ($\omega = 1.0$) with normalized wave number $\kappa_c a = 0.125$ and 0.913, respectively. Figures 6–7 show the total displacement components along the principal cut at the surface. The solutions are also very close to the analytical solutions.

For the generalized case with both the host medium and obstacle being elastic, we select $\lambda = 0.53486$, $\mu = 0.23077$ and $\rho = 1.0$ for the host medium, and $\lambda_0 = 0.23716$, $\mu_0 = 0.52641$ and $\rho_0 = 1.9852$ for the elastic spherical inclusion with unit radius. Figures 8–9 plot the tangential or radial components of the total traction and displacement at the surface along the principal cut for $\kappa_c a = 0.125$ and 0.913. These results are also in excellent agreement with the analytical solutions.

We choose spherical objects as scatterers because there are available analytical solutions to compare in numerical solutions for scattering by such objects. MoM can of course be used to solve the scattering by arbitrarily shaped objects and Figure 10 is an illustration of the solutions of scattering by an elastic cube with a side length of $2a$. We calculate the scattered displacement

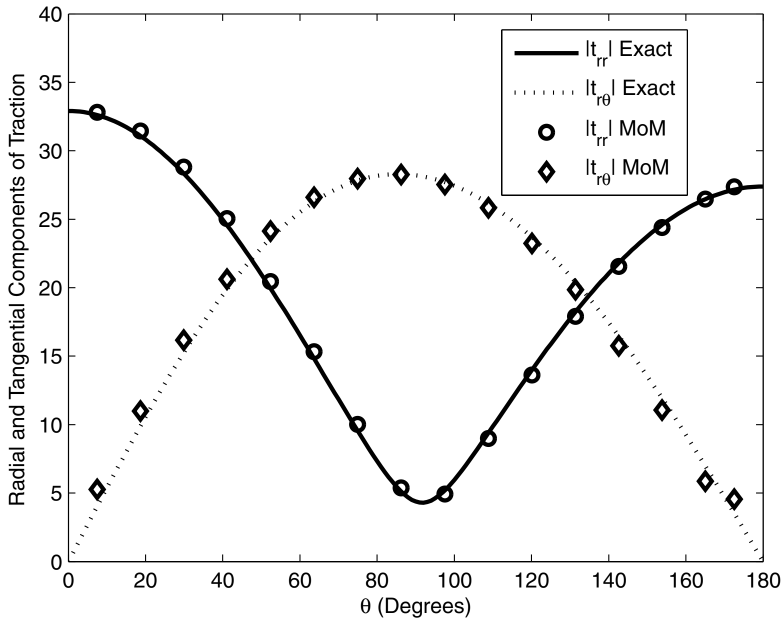

Figure 3. Radial and tangential components of total traction along the principal cut at the surface of a rigid sphere, $k_c a = 0.125$.

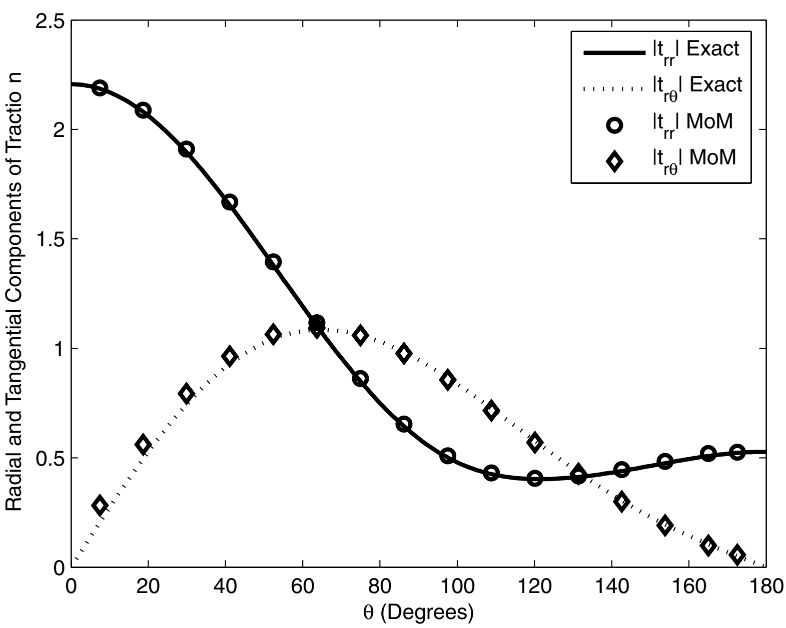

Figure 4. Radial and tangential components of total traction along the principal cut at the surface of a rigid sphere, $k_c a = 0.913$.

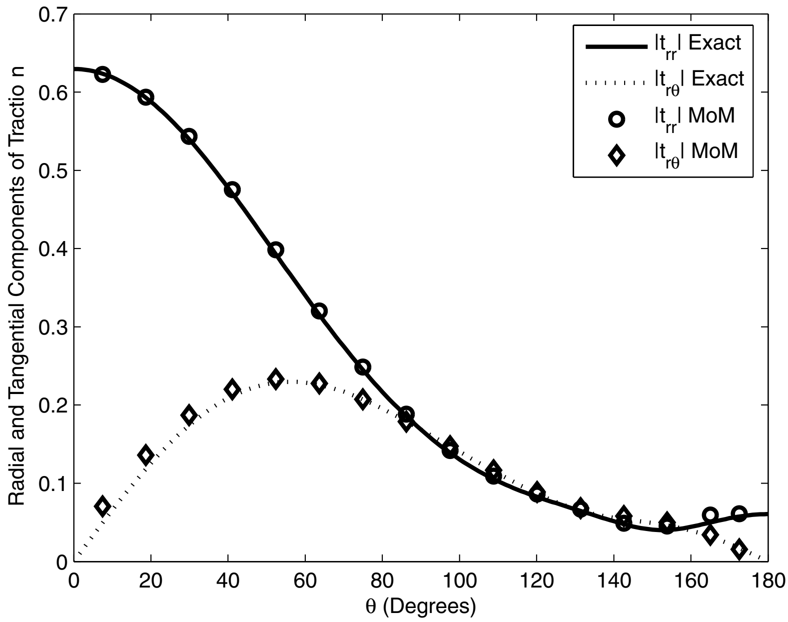

Figure 5. Radial and tangential components of total traction along the principal cut at the surface of a rigid sphere, $k_c a = \pi$.

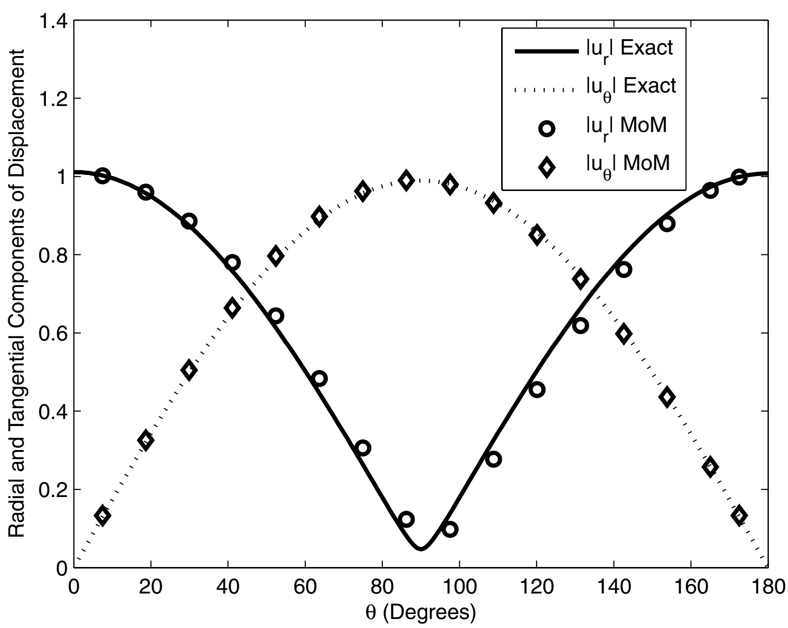

Figure 6. Radial and tangential components of total displacement along the principal cut at the surface of a cavity, $k_c a = 0.125$.

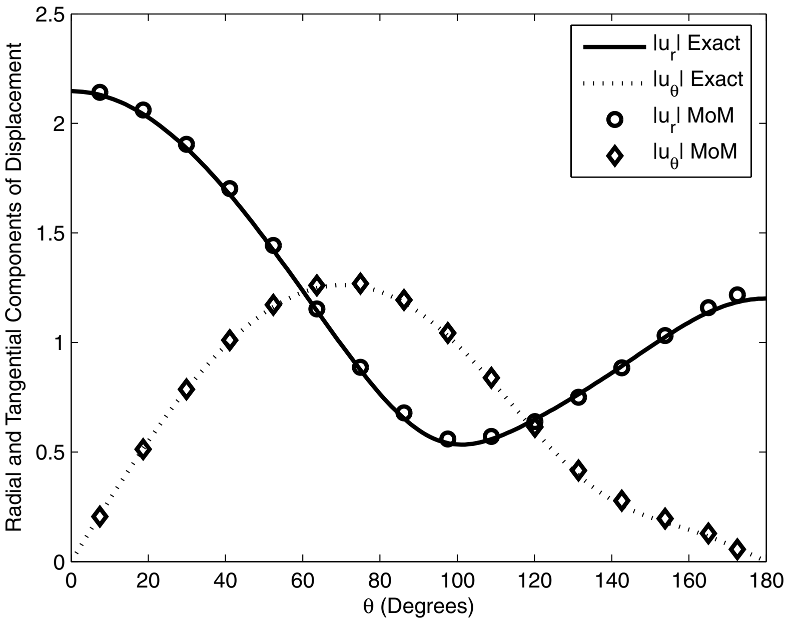

Figure 7. Radial and tangential components of total displacement along the principal cut at the surface of a cavity, $k_c a = 0.913$.

field at the $r = 5a$ surface along the principal cut under the same material properties and incident wave as in the generalized case.

6.2. *Acoustic wave scattering*

In principle, the acoustic wave equation can be derived from the elastic wave equation by letting $\mu \to 0$ as shown in Sections 3 and 4. The shear wave part of the dyadic Green's function becomes a Dirac delta distribution as shown by Equation (13). However, from our numerical experimentation, it is difficult to achieve this numerically by setting $\mu \to 0$, as the Green's function for the shear wave becomes highly oscillatory. This oscillation makes the numerical evaluation of the matrix elements difficult. We have also experimented with $\mu = -i\delta$ where δ is a small number. This is analogous to the highly conductive medium case in electromagnetics, where the shear wave will be highly attenuated. However, an oscillatory factor of the Green's function still persists with this choice making its accurate numerical evaluation difficult.

We find that the best approach is to let $\mu = -\delta$ where δ is a small number. This is analogous to a plasma medium in electromagnetics where waves become evanescent with no oscillatory component, or are shielded in a short length-scale.

In the following, the acoustic wave scattering solution can be derived numerically using the original elastic wave BIE with a negative small value of μ. This approach allows one to solve for the scattering of both waves in a unified manner using one numerical code. Figure 11 shows the solutions of scattering by a rigid sphere with $a = 1.0$, $\rho = 1.0$, $\omega = 1.0$ and $\kappa_c a = 1.0$. We take $\mu = -10^{-3}$ for this case and the solution is very close to the analytical counterpart. It can be seen that the $\mu = -10^{-3}$ solution approximates the $\mu = 0$ solution. On the other hand, the

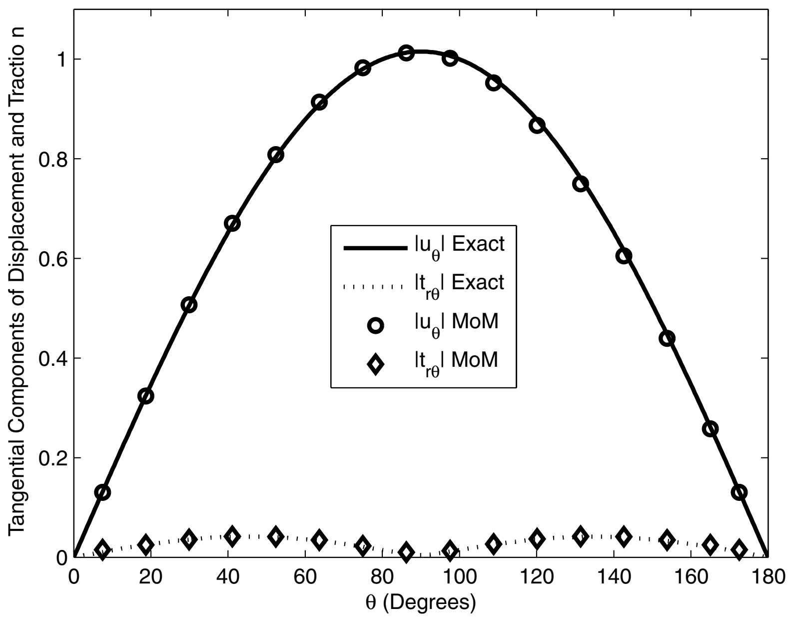

Figure 8. Tangential components of total displacement and traction along the principal cut at the surface of an elastic sphere, $k_c a = 0.125$.

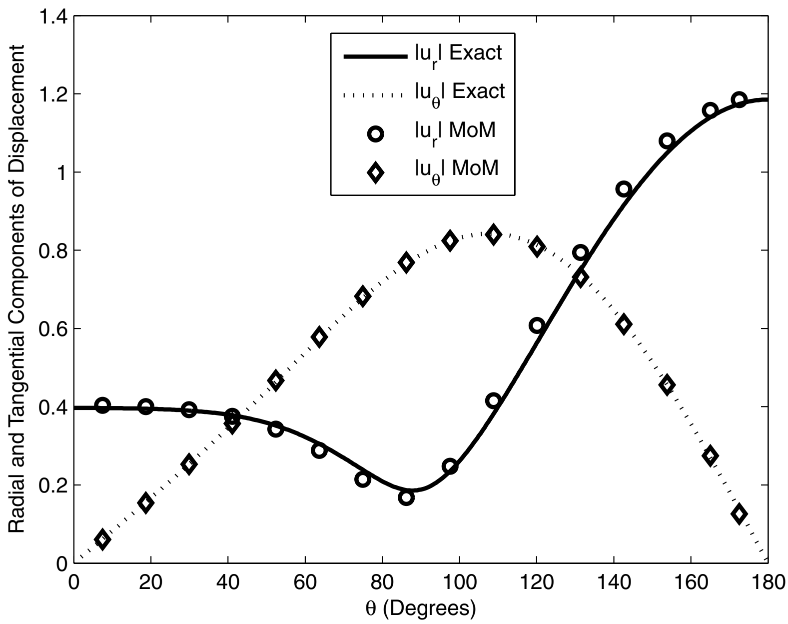

Figure 9. Radial and tangential components of total displacement along the principal cut at the surface of an elastic sphere, $k_c a = 0.913$.

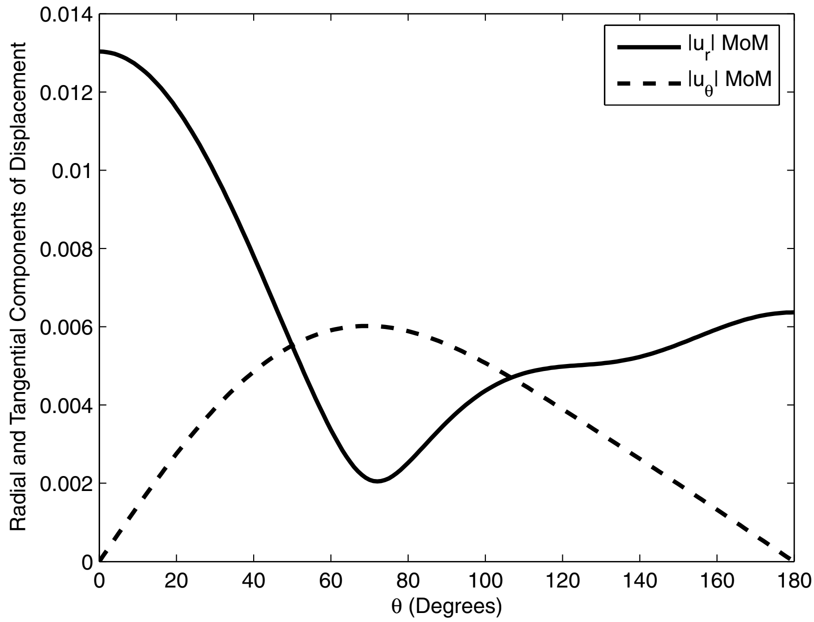

Figure 10. Radial and tangential components of scattered displacement along the principal cut at the $r = 5a$ surface by an elastic cube, $k_c a = 0.125$.

$\mu = 10^{-3}$ solution approximates the $\mu = 0$ case with difficulty and less accurately due to the highly oscillatory integral kernels.

Figure 12 illustrates the scattering by an elastic sphere with the same parameters as the rigid sphere case except the penetrable property of the sphere now. The elasticity of the sphere is the same as the third case for the elastic wave scattering. The numerical solution is also in good agreement with the analytical one for the smaller value of μ and also the approximation between negative μ and $\mu = 0$ gets better if μ is closer to 0.

If μ is exactly equal to 0, we need to use the vector BIE (15) to solve for acoustic wave scattering. Similar to the elastic wave scattering, we consider the scattering by a rigid sphere, a spherical cavity and an elastic sphere, all with unit radius, respectively. For the rigid sphere case, the host medium is characterized by $\rho = 1.0$, $\mu = 0$ and λ which is determined by other parameters. The incident wave has a unit circular frequency ($\omega = 1.0$) and normalized wave number of $\kappa_c a = 0.5$ and π, respectively. Figures 13–14 show the radial components of total traction along the principal cut at the surface of the rigid sphere. Since there is no shear wave, the tangential component of traction is zero. It can be seen that the MoM solutions are very close to the analytical solutions.

For the spherical cavity case, the host medium and incident wave are the same as before except $\kappa_c a = 0.913$ now. The numerical and analytical solutions are shown in Figure 15 and a good agreement is seen again.

Finally, for the elastic inclusion case, we choose the same parameters as in the preceding elastic wave scattering, except $\mu = 0$ for the host medium now. Figure 16 plots the solutions for $\kappa_c a = 0.913$ and they are also consistent with the analytical results.

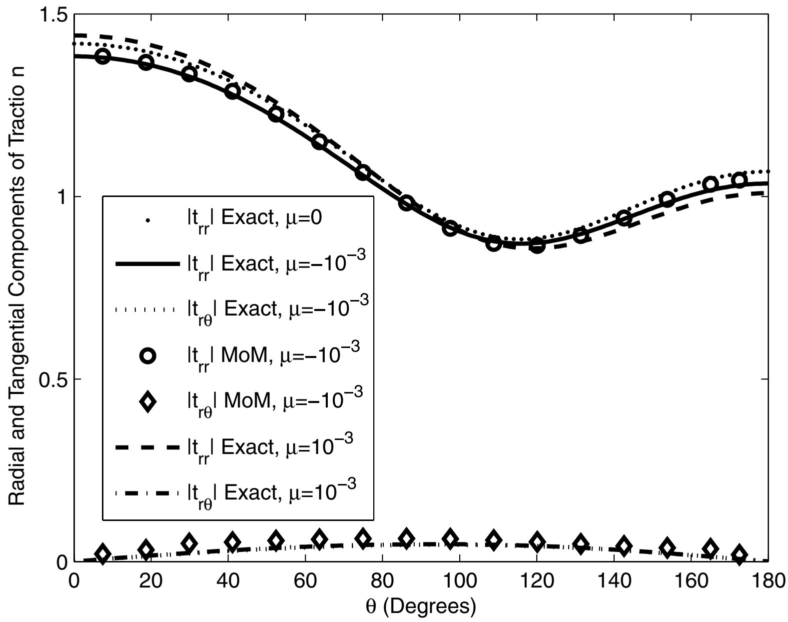

Figure 11. Radial and tangential components of total traction along the principal cut at the surface of a rigid sphere with a small value of μ.

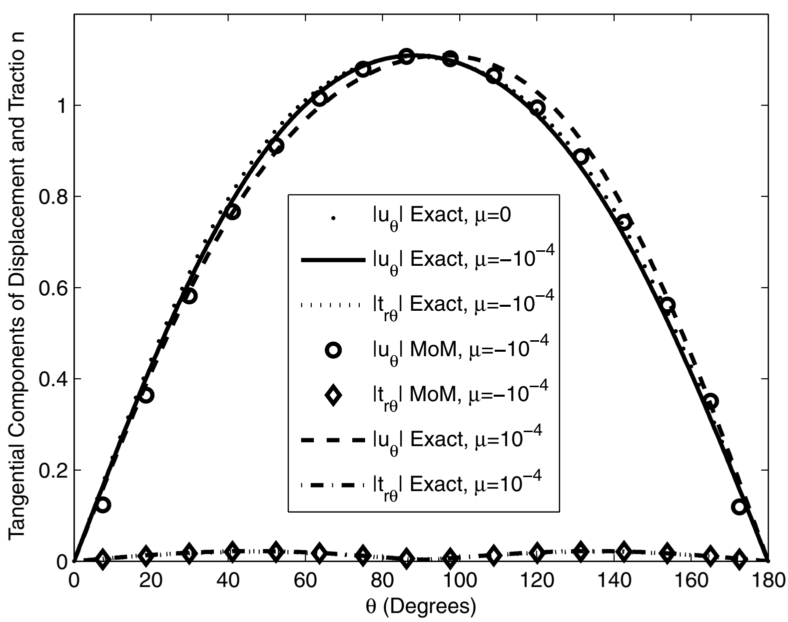

Figure 12. Tangential components of total displacement and traction along the principal cut at the surface of an elastic sphere with a small value of μ.

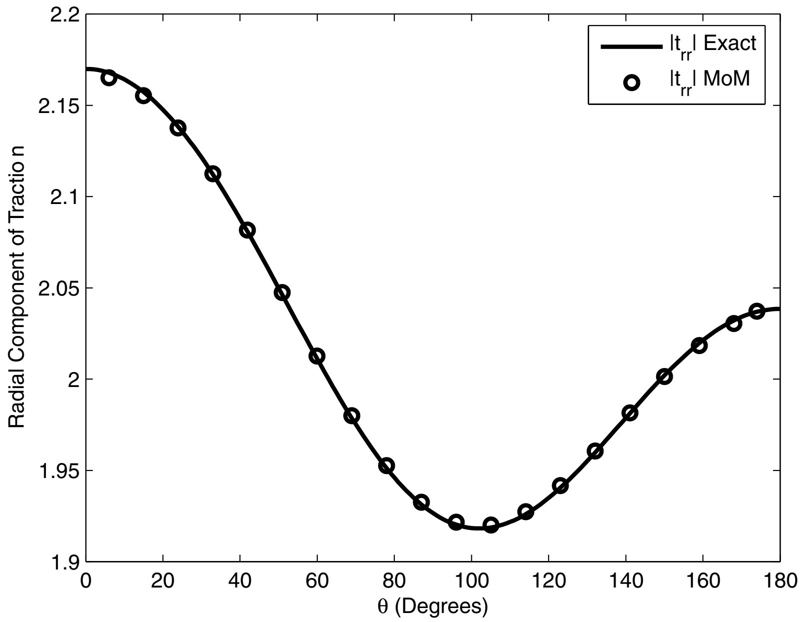

Figure 13. Radial components of total traction along the principal cut at the surface of a rigid sphere, $k_c a = 0.5$.

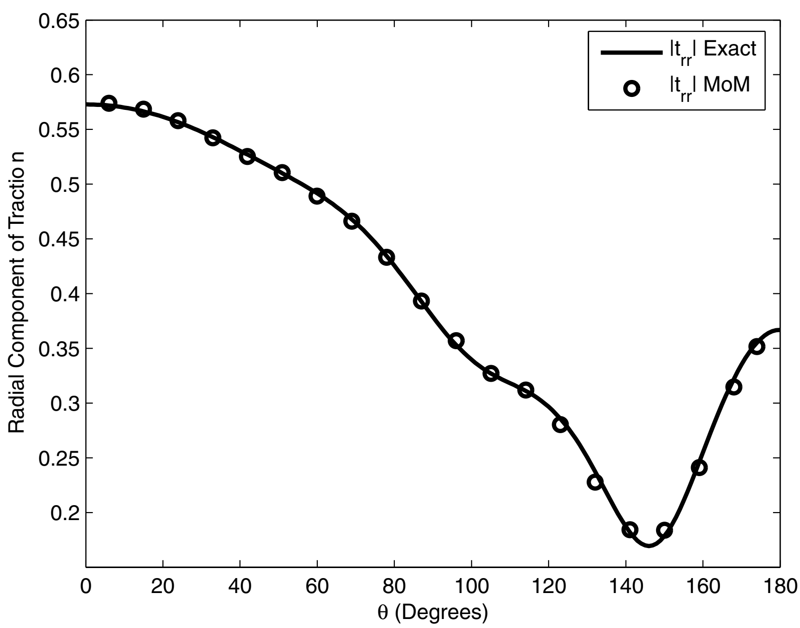

Figure 14. Radial components of total traction along the principal cut at the surface of a rigid sphere, $k_c a = \pi$.

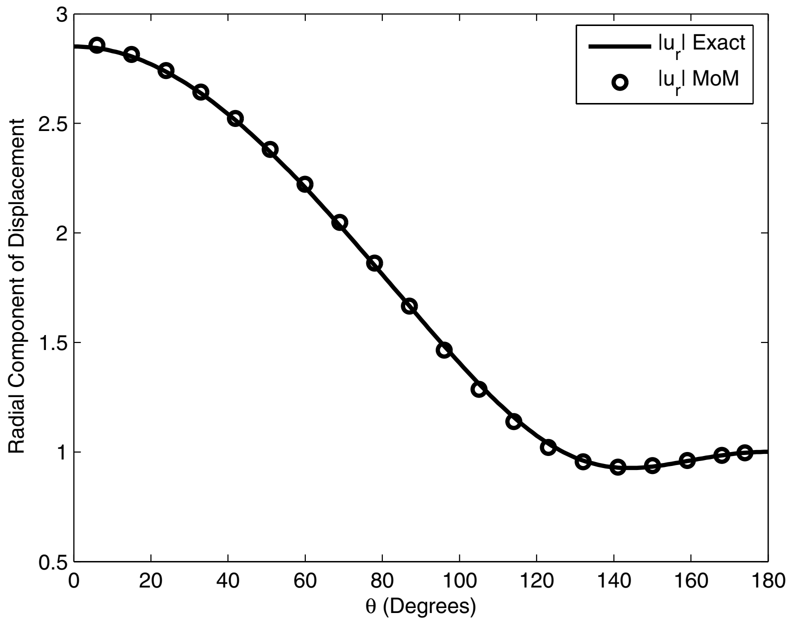

Figure 15. Radial components of total displacement along the principal cut at the surface of a spherical cavity, $k_c a = 0.913$.

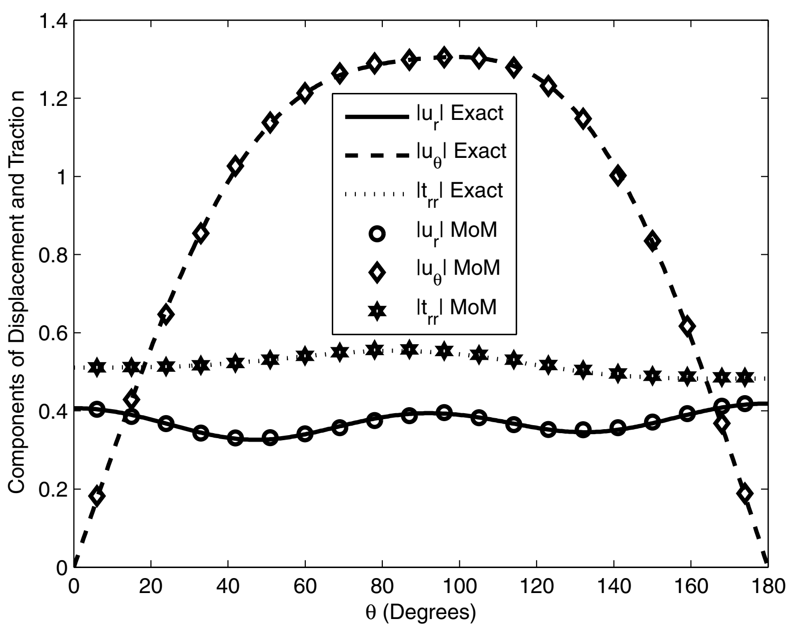

Figure 16. Radial and tangential components of total displacement and traction along the principal cut at the surface of an elastic sphere, $k_c a = 0.913$.

7. Conclusions

We have developed a unified form of boundary integral equation for the scattering of elastic and acoustic waves. Under this unified form, acoustic wave scattering can be solved for using the vector elastic wave BIE either by introducing a shielding loss for a small shear modulus. In this manner, only one numerical code needs to be maintained from which acoustic wave scattering solutions and elastic wave scattering solutions can be derived.

We also show that by using the derived limit of the Green's tensor for a zero shear modulus, an alternative way of solving the acoustic wave scattering problem using vector fields is possible. Even though this added complication is unnecessary, it can be shown that solving this equation is exactly equivalent to solving the scalar acoustic wave equation. The new approach has the same complexity as the traditional scalar BIE. Although the scalar BIE is simpler in implementation, the vector BIE provides extra information about the displacement in addition to the velocity potential. This is desirable in some cases, such as in fluid or underwater acoustics.

In terms of our literature search, the MoM presented here has been used for the first time to solve the elastic wave BIE. Since the 3D unknown functions are defined over a surface in the BIE, we divide the unknown functions into normal components and tangential components, and expand them using the pulse basis and RWG basis, respectively. The discretized BIE is then tested with these basis functions, yielding a Galerkin scheme. Since MoM enforces the boundary conditions to be satisfied in a better manner, it is more stable, more accurate, and uses fewer unknowns compared with collocation-based methods with the same discretization.

Acknowledgment

This work was supported by CERL, US Army under grant W9132T-06-2-0006.

References

[1] Y.-H. Chen, W.C. Chew, and Q.H. Liu, *A three-dimensional finite difference code for the modeling of sonic logging tools*, J. Acoust. Soc. Amer. 93 (1998), pp. 702–712.

[2] W.C. Chew and Q.H. Liu, *Perfectly matched layers for elastodynamics: A new absorbing boundary condition*, J. Comp. Acoust. 4 (1996), pp. 341–359.

[3] C.J. Randall, *Absorbing boundary condition for the elastic wave equation: velocity–stress formulation*, Geophys. 54 (1989), pp. 1141–1152.

[4] W.M. Visscher, *A new way to calculate scattering of acoustic and elastic waves I. Theory illustrated for scalar waves*, J. Appl. Phys. 51 (1980), pp. 825–834.

[5] P.S. Kondapalli and D.J. Shippy, *Analysis of acoustic scattering in fluids and solids by the method of fundamental solutions*, J. Acoust. Soc. Amer. 91 (1992), pp. 1844–1854.

[6] A. Boström, *Scattering of stationary acoustic waves by an elastic obstacle immersed in a fluid*, J. Acoust. Soc. Amer. 67 (1980), pp. 390–398.

[7] A. Boström, *Scattering of acoustic waves by a layered elastic obstacle in a fluid – An improved null field approach*, J. Acoust. Soc. Amer. 76 (1984), pp. 588–593.

[8] R. Lim, *Acoustic scattering by a partially buried three-dimensional elastic obstacle*, J. Acoust. Soc. Amer. 104 (1998), pp. 769–782.

[9] A. Boag, Y. Leviatan, and A. Boag, *Analysis of two-dimensional acoustic scattering from periodic structures using a hybrid source model*, J. Acoust. Soc. Amer. 86 (1989), pp. 387–394.

[10] C.A. Balanis, *Advanced Engineering Electromagnetics*, John Wiley, New York, 1989.

[11] Y. Shi and U.S. Shirahatti, *The use of the method of moments with finite difference operator in acoustics*, J. Acoust. Soc. Amer. 99 (1996), pp. 2667–2673.

[12] S.M. Rao and B.S. Sridhara, *Acoustic scattering from arbitrarily shaped multiple bodies in half-space: Method of moments solution*, J. Acoust. Soc. Amer. 91 (1992), pp. 652–657.

[13] S.M. Rao and B.S. Sridhara, *Application of the method of moments to acoustic scattering from arbitrary shaped rigid bodies coated with lossless, shearless materials of arbitrary thickness*, J. Acoust. Soc. Amer. 90 (1991), pp. 1601–1607.
[14] S.M. Rao and P.K. Raju, *Application of the method of moments to acoustic scattering from multiple bodies of arbitrary shape*, J. Acoust. Soc. Amer. 86 (1989), pp. 1143–1148.
[15] F.H. Fenlon, *Calculation of the acoustic radiation field at the surface of a finite cylinder by the method of weighted residuals*, Proc. IEEE 57 (1969), pp. 291–306.
[16] N.J. De Lautour, *A Galerkin method for the numerical analysis of diffraction by a rectangular screen*, J. Acoust. Soc. Amer. 106 (1999), pp. 3072–3080.
[17] R.R. Erickson and B.T. Zinn, *Modeling of finite amplitude acoustic waves in closed cavities using the Galerkin method*, J. Acoust. Soc. Amer. 113 (2003), pp. 1863–1870.
[18] Y. Ding, A. Forestier, and T. Ha Duong, *A Galerkin scheme for the time domain integral equation of acoustic scattering from a hard surface*, J. Acoust. Soc. Amer. 86 (1989), pp. 1566–1572.
[19] S.M. Rao, D.R. Wilton, and A.W. Glisson, *Electromagnetic scattering by surfaces of arbitrary shape*, IEEE Trans. Antennas Propagat. 30 (1982), pp. 409–418.
[20] M.S. Tong and W.C. Chew, *A direct approach for solving 3D EFIE with double gradient of the Green's function*, Proc. IEEE Antennas Propagat. Soc. Int. Symp. 4 (2006), pp. 2855–2858.
[21] Y.H. Pao and V. Varatharajulu, *Huygens' principle, radiation conditions, and integral formulas for the scattering of elastic waves*, J. Acoust. Soc. Amer. 59 (1976), pp. 1361–1371.
[22] F.J. Rizzo, D.J. Shippy, and M. Rezayat, *A boundary integral equation method for radiation and scattering of elastic waves in three dimensions*, Int. J. Numer. Methods Eng. 21 (1985), pp. 115–129.
[23] P.S. Kondapalli, D.J. Shippy, and G. Fairweather, *The method of fundamental solutions for transmission and scattering of elastic waves*, Comput. Methods Appl. Mech. Eng. 96 (1992), pp. 255–269.
[24] W.C. Chew, *Elastic Wave Lecture Notes, ECE471*, University of Illinois at Urbana-Champaign, USA, 1991.
[25] W.C. Chew, *Waves and Fields in Inhomogeneous Media*, Van Nostrand Reinhold, New York, 1990. (Reprinted by IEEE Press, New York, 1995.)
[26] Y.-H. Pao and C.C. Mow, *Scattering of plane compressional waves by a spherical obstacle*, J. Appl. Phys. 34 (1963), pp. 493–499.
[27] A.F. Seybert, B. Soenarko, F.J. Rizzo, and D.J. Shippy, *An advanced computational method for radiation and scattering of acoustic waves in three dimensions*, J. Acoust. Soc. Amer. 77 (1985), pp. 362–368.
[28] E. Skudrzyk, *The Foundations of Acoustics*, Springer-Verlag, New York, 1971.
[29] P.M. Morse and H. Feshbach, *Methods of Theoretical Physics*, McGraw-Hill, New York, 1953.

Appendix A:

Analytical solutions for spherical obstacles

Both elastic wave and acoustic wave scattering by a spherical obstacle have analytical solutions and they are usually used as a benchmark to verify numerical results. Although Pao and Mow provided the general solutions for elastic wave scattering [26], the asymptotic solutions for acoustic wave scattering are not available; hence we present the results here. For a rigid sphere, the solution for the total traction field is

$$\begin{aligned} \tau_{rr} &= \frac{2\mu}{r^2}\sum_{n=0}^{\infty}(-\Phi_0\mathcal{E}_3 + A_n\mathcal{E}_{31} + B_n\mathcal{E}_{32})P_n(\cos\theta) \\ \tau_{r\theta} &= \frac{2\mu}{r^2}\sum_{n=0}^{\infty}(-\Phi_0\mathcal{E}_4 + A_n\mathcal{E}_{41} + B_n\mathcal{E}_{42})\frac{P_n(\cos\theta)}{d\theta} \end{aligned} \tag{A1}$$

where we have used the notation in [26]. Here, τ is the traction vector, Φ_0 is the amplitude of the incident plane compressional wave travelling in the x_3 direction, P_n is the Legendre polynomial of order n, A_n and B_n are the coefficients to be determined, and all $\mathcal{E}$'s are defined in (18) in [26]. In the limit of $\mu \to 0$, we have

$$\lim_{\mu\to 0}\mu\mathcal{E}_3 = \frac{1}{2}i^{-n}(2n+1)\omega^2\rho r^2 j_n(\alpha r) = \mathcal{E}_3^0$$
$$\lim_{\mu\to 0}\mu\mathcal{E}_{31} = -\frac{1}{2}\omega^2\rho r^2 h_n(\alpha r) = \mathcal{E}_{31}^0 \tag{A2}$$

and all other terms incorporating μ will be zero. Here j_n is the spherical Bessel function of order n, h_n is the spherical Hankel function of the first kind of order n and α is the wave number of the compressional wave in the host medium. Thus the solution reduces to

$$\tau_{rr} = \frac{2}{r^2}\sum_{n=0}^{\infty}\Big(-\Phi_0\mathcal{E}_3^0 + A_n\mathcal{E}_{31}^0\Big)P_n(\cos\theta)$$
$$\tau_{r\theta} = 0 \tag{A3}$$

with

$$A_n = \Phi_0\frac{E_1}{E_{11}} = -\Phi_0 i^{-n}(2n+1)\frac{nj_n(\alpha a) - \alpha a j_{n+1}(\alpha a)}{nh_n(\alpha a) - \alpha a h_{n+1}(\alpha a)} \tag{A4}$$

where E is the value of $\mathcal{E}$ at $r = a$ and a is the radius of the sphere. This solution, when only considering the scattered part, is the same as the conventional analytical solution for the scattered potential by a rigid sphere in acoustics [27]

$$\Phi_s(r,\theta) = \Phi_i\sum_{m=0}^{\infty} i^{m+1}(2m+1)P_m(\cos\theta)\sin\delta_m(\kappa a)h_m(\kappa r)e^{i\delta_m(\kappa a)} \tag{A5}$$

if we note that $\tau = \hat{n}\lambda\nabla\cdot u = \hat{n}\lambda\Phi$. The notation in (A5) can be found in [28] and $\delta_m(z)$ is the phase of $\frac{d}{dz}h_m(z)$ minus $\frac{\pi}{2}$.

For an elastic inclusion, we can derive the following equations from Equation (20) in [26] by taking the limit $\mu \to 0$

$$E_{11}A_n + E_{13}C_n + E_{14}D_n = \Phi_0 E_1$$
$$E_{31}^0 A_n + E_{33}C_n + E_{34}D_n = \Phi_0 E_3^0$$
$$E_{43}C_n + E_{44}D_n = 0 \tag{A6}$$

where E_3^0 and E_{31}^0 are $\mathcal{E}_3^0$ and $\mathcal{E}_{31}^0$ with $r = a$ in (A2), respectively. With the solved coefficients from (A6), the analytical solutions are

$$u_r = \frac{1}{r}\sum_{n=0}^{\infty}(-\Phi_0\mathcal{E}_1 + A_n\mathcal{E}_{11})P_n(\cos\theta)$$
$$u_\theta = \frac{1}{r}\sum_{n=0}^{\infty}(-\Phi_0\mathcal{E}_2 + A_n\mathcal{E}_{21})\frac{dP_n(\cos\theta)}{d\theta}$$
$$\tau_{rr} = \frac{2}{r^2}\sum_{n=0}^{\infty}\Big(-\Phi_0\mathcal{E}_3^0 + A_n\mathcal{E}_{31}^0\Big)P_n(\cos\theta)$$
$$\tau_{r\theta} = 0. \tag{A7}$$

Similarly, we can find the following analytical solution for acoustic scattering by a traction-free cavity

$$u_r = \frac{1}{r}\sum_{n=0}^{\infty}(-\Phi_0\mathcal{E}_1 + A_n\mathcal{E}_{11})P_n(\cos\theta)$$
$$u_\theta = 0 \tag{A8}$$

where

$$A_n = \Phi_0\frac{E_3^0}{E_{31}^0} = -\Phi_0 i^{-n}(2n+1)\frac{j_n(\alpha a)}{h_n(\alpha a)}. \tag{A9}$$